Elastic Bounded Diffusion and Electron Propagation: Dynamics of the Wiring of a Self-Assembly of Immunoglobulins Bearing Terminally Attached Ferrocene Poly(ethylene glycol) Chains According to a Spatially Controlled Organization

Agnès Anne, Christophe Demaille, and Jacques Moiroux*

Contribution from the Laboratoire d'Electrochimie Moléculaire, Unité Mixte de Recherche Université - CNRS No 7591, Université de Paris 7 - Denis Diderot, 2 place Jussieu, 75251 Paris Cedex 05, France

Received November 22, 2000

Abstract: Molecular monolayers of immunoglobulins bearing terminally attached ferrocene poly(ethylene glycol) chains (IgG−PEG−Fc) were self-assembled at an electrode surface in a step-by-step manner involving antigen−antibody recognition reactions. The total number N of assembled IgG−PEG−Fc monolayers and the number of spacers n_i separating two successive IgG−PEG−Fc monolayers were controlled and varied. Electron transport through the protein assembly involves the dynamics of the terminally attached PEG chains and isotopic electron exchange between ferrocene heads belonging to successive IgG−PEG−Fc monolayers. The model of elastic bounded diffusion enabled us to analyze quantitatively the dependence of the rate of electron transport on N, n_i, and the rate constant (k_e) of isotopic electron exchange. Wiring of a molecular monolayer of redox enzyme is also quantitatively characterized.

Introduction

In a previous study,[1] we showed that bioconjugates of globular immunoglobulins (IgG) bearing terminally attached poly(ethylene glycol) (PEG) chains with ferrocene (Fc) heads could be prepared rather easily by reaction of amino groups of the protein with linear NHS−PEG−Fc molecules, NHS being an *N*-hydroxysuccinimide activated ester, provided that the NHS−PEG−Fc reagent is available.[1,2] The loose end of the linear chain is linked to the ferrocene head, a redox label which is small and only slightly solvent-sensitive.[3] On average, up to ca. 20 PEG−Fc linear chains could be attached to a single IgG molecule with preservation of the immunological activity of the latter.[1] One molecular monolayer of PEG−Fc-labeled IgG (IgG−PEG−Fc) was self-assembled at an electrode surface on top of various constructions of successively self-assembled molecular monolayers of adequately chosen IgG's from different sources so as to vary the distance at which the IgG−PEG−Fc monolayer is located away from the electrode surface, and we showed that a transient technique like cyclic voltammetry could be used to characterize quantitatively the dynamics of the PEG chains in such structures made of self-assembled proteins. To explain the observed behavior we proposed a model of bounded elastic diffusion.[1]

The present work deals with the wiring of a much larger self-assembly of successive IgG molecular monolayers, some of them being monolayers of IgG−PEG−Fc. Within the structure, the distance separating two successive IgG−PEG−Fc monolayers can be controlled and thus shortened or lengthened. Besides the dynamics of the PEG chains, electron propagation from the electrode to the various regions of the whole assembly will then depend on the rate of electron self-exchange between the Fc heads of PEG−Fc chains anchored in two successive IgG−PEG−Fc monolayers. Owing to the limited length of the PEG linear chain the Fc heads linked to the second monolayer of IgG−PEG−Fc bioconjugate cannot reach the electrode; therefore, efficient wiring requires that the Fc heads linked to the second IgG−PEG−Fc monolayer can actually exchange electrons with the Fc heads linked to the first IgG−PEG−Fc monolayer which are precisely the ones which can reach the electrode surface. Connection to the third IgG−PEG−Fc monolayer implies that the Fc heads attached to it can exchange electrons with the Fc heads linked to the second IgG−PEG−Fc monolayer and so on. The parameters controlling the time response of the wired molecular assembly are identified, and the dependence of the kinetics of the system on each parameter is quantitatively characterized. Compared to polymeric films containing covalently linked redox sites,[4] or dendritic structures bearing peripheral redox sites,[5] within which apparent diffusion of electrons was quantitatively examined, the system under study in the present work contains much smaller concentrations of redox sites but they can move over much wider distances and, most of all, their spatial distribution can be varied significantly through the control of structural parameters.

(1) Anne, A.; Demaille, C.; Moiroux, J. *J. Am. Chem. Soc.* **1999**, *121*, 10379−10388.

(2) (a) Anne, A. *Tetrahedron Lett.* **1998**, *39*, 561−564. (b) Anicet, N.; Anne, A.; Moiroux, J.; Savéant, J.-M. *J. Am. Chem. Soc.* **1998**, *120*, 7115−7116. (c) Anne, A.; Moiroux, J. *Macromolecules* **1999**, *32*, 5829−5835.

(3) Hupp, J. T. *Inorg. Chem.* **1990**, *29*, 5010−5012.

(4) (a) Dahms, H. J. *J. Phys. Chem.* **1968**, *72*, 362−364. (b) Ruff, I.; Friedrich, V. J. *J. Phys. Chem.* **1971**, *75*, 3297−3302. (c) Ruff, I.; Friedrich, V. J.; Demeter, K.; Csillag, K. *J. Phys. Chem.* **1971**, *75*, 3303−3309. (d) Andrieux, C. P.; Savéant, J.-M. *J. Electroanal. Chem.* **1980**, *111*, 377−381. (e) Laviron, E. *J. Electroanal. Chem.* **1980**, *112*, 1−9. (f) Andrieux, C. P.; Savéant, J.-M. Catalysis at redox polymer coated electrodes. In *Molecular Design of Electrode Surfaces*, *Techniques in Chemistry*; Murray, R. W., Ed.; Wiley: New York, 1992; Vol. 22, pp 207−270. (g) Blauch, D. N.; Savéant, J.-M. *J. Am. Chem. Soc.* **1992**, *114*, 3323−3332. (h) Blauch, D. N.; Savéant, J.-M. *J. Phys. Chem.* **1993**, *97*, 6444−6448.

(5) Amatore, C.; Bouret, Y.; Maisonhaute, E.; Goldsmith, J. I.; Abruna, H. D. *Chem. Phys. Chem.* **2001**, *2*, 130−134.

10.1021/ja004050f CCC: $20.00
Published on Web 04/27/2001

Electrical wiring of redox enzymes is a permanent goal for the achievement of integrated systems in which the biocatalyst and the redox mediator which conveys electrons between the electrode surface and the enzyme active site are both incorporated in the modified electrode.[6] Besides the rate of reaction of the enzyme with its substrate, the efficiency of such an integrated system depends a priori on both the kinetics of electron transport through the matrix and the rate at which the incorporated mediator reacts with the enzyme. After immunological attachment of a monolayer of glucose oxidase on top of the wired molecular assembly,[7] we also characterized quantitatively the catalytic efficiency and identified the parameters controlling the kinetics of the system.

Results and Discussion

Construction of the Wired Self-Assembly of Proteins. The IgG−PEG−Fc bioconjugate was prepared by covalent grafting of NHS−PEG−Fc chains to an anti-goat IgG produced in mouse through reaction of the NHS activated ester with accessible amino groups of the immunoglobulin.[8] ICP-MS assays of iron showed that the degree of PEG−Fc labeling was reproducible for a given source of IgG and could reach 17.[1]

The IgG self-assemblies were constructed on glassy carbon electrodes by successive immobilization of an adequate sequence of monolayers of polyclonal antibodies, according to already reported procedures[7] and as described in the Experimental Section. A sketch of the resulting structure is given in Figure 1. The first molecular monolayer is made of adsorbed whole anti-mouse IgG produced in goat (GtxMo). Gelatin was adsorbed at the glassy carbon surface to prevent nonspecific binding. A whole anti-goat IgG produced in mouse (MoxGt) with minimal cross-reactivity to mouse, human, and rabbit serum proteins was used for the synthesis of the IgG−PEG−Fc bioconjugate.[1] Attachment of the first monolayer of IgG−PEG−Fc results from molecular recognition of the adsorbed monolayer of (GtxMo) by the synthesized IgG−PEG−Fc bioconjugate.

Immunological reaction of the IgG−PEG−Fc monolayer with (GtxMo) was then used for the construction of IgG self-assemblies in which two successive IgG−PEG−Fc monolayers were separated by only one monolayer of whole antibodies bearing no PEG−Fc chains and acting as a spacer ($n_i = 1$ in Figure 1b). Then the attachment of the second IgG−PEG−Fc monolayer resulted from the same immunological reaction as the one involved in the immobilization of the first IgG−PEG−Fc monolayer. Attachments of following IgG−PEG−Fc monolayers, separated by one whole IgG spacer, were carried out by repeating the procedure up to the self-assembly of the desired total number (N) of IgG−PEG−Fc monolayers.

For the construction of IgG self-assemblies of IgG−PEG−Fc monolayers separated by more than one whole IgG spacer, we proceeded as follows. The last attached IgG−PEG−Fc monolayer was recognized by a whole anti-mouse IgG produced in rabbit (RbxMo). For $n_i = 2$, the immobilized molecular monolayer of (RbxMo) was recognized by a whole anti-rabbit IgG produced in goat (GtxRb) which is suited for immunological attachment of the following (MoxGt) IgG−PEG−Fc monolayer as sketched in Figure 1b. For $n_i = 1.5$, a Fab fragment of (GtxRb) was used instead of the whole (GtxRb) antibody to introduce the equivalent of a half-size spacer as illustrated in Figure 1c. The one half-space equivalence was established in our previous work.[1] Immobilization of the enzyme molecular monolayer on top of the Nth IgG−PEG−Fc monolayer was achieved by immunological reaction of glucose oxidase conjugated whole (GtxMo) antibody.

It is worth pointing out that the binding of each new monolayer relies on molecular recognition of the outermost monolayer of the already assembled structure by antibodies which are introduced in solution. Therefore, the antibodies are oriented within the assembly in such a way that their sub-

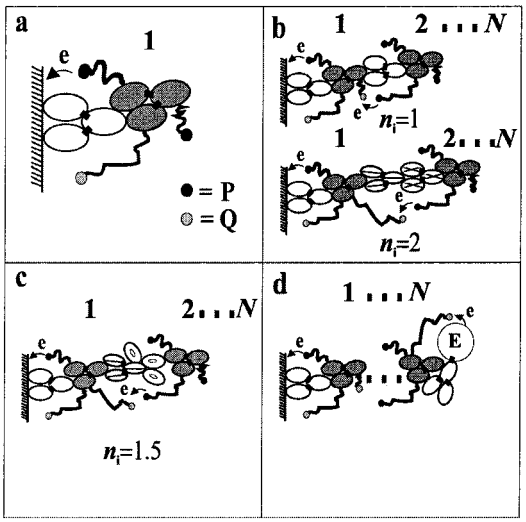

Figure 1. Immunological self-assembly of the PEG−Fc wired system of immobilized proteins. P = Fc and Q = Fc^+ are respectively the reduced or oxidized heads of the PEG (MW 3400 g/mol) chains covalently attached to the IgG protein of the IgG−PEG−Fc bioconjugate. (a) immobilization of the first IgG−PEG−Fc monolayer (N = 1) obtained by adsorption of a monolayer of whole (GtxMo)IgG (white filling in the sketch) followed by immunological attachment of the (MoxGt)IgG−PEG−Fc bioconjugate (dark gray filling). (b) Immobilization of N (MoxGt)IgG−PEG−Fc monolayers separated by n_i = 1 or 2 intermediate monolayers of whole IgG's. For $n_i = 1$, a monolayer of whole (GtxMo) antibodies (white filling) is immunologically attached on top of the preceding (MoxGt)IgG−PEG−Fc monolayer and then recognized by a new (MoxGt)IgG−PEG−Fc monolayer (dark gray filling). For $n_i = 2$, the preceding (MoxGt)IgG−PEG−Fc monolayer is recognized by a monolayer of whole (RbxGt) antibodies (one straight line filling) which is consecutively recognized by a monolayer of whole (GtxRb) antibodies (cross filling), the latter allowing immunological attachment of the following (MoxGt)IgG−PEG−Fc monolayer (dark gray filling). (c) Immobilization of N IgG−PEG−Fc monolayers separated by one monolayer of whole IgG antibodies plus one monolayer of Fab fragments so as to obtain n_i = 1.5. The preceding (MoxGt)IgG−PEG−Fc monolayer is recognized by a monolayer of whole (RbxGt) antibodies (one straight line filling) which is consecutively recognized by a monolayer of (GtxRb) Fab fragments (ellipsoid filling), the latter allowing immunological attachment of the following (MoxGt)IgG−PEG−Fc monolayer (dark gray filling). (d) Immobilization of the enzyme whole (GtxMo) antibody (white filling) conjugate (E = glucose oxidase in the sketch). The definitions of (GtxMo), (MoxGt), (RbxGt), and (GtxRb) are given in the text.

(6) (a) Heller, A. *Acc. Chem. Res.* **1990**, *23*, 128−134. (b) Heller, A. *J. Phys. Chem.* **1992**, *96*, 3579−3587. (c) Aoki, A.; Heller, A. *J. Phys. Chem.* **1993**, *97*, 11014−11019. (d) Katakis, I.; Ye, L.; Heller, A *J. Am. Chem. Soc.* **1994**, *116*, 3617−3618.

(7) (a) Bourdillon, C.; Demaille, C.; Gueris, J.; Moiroux, J.; Savéant, J.-M. *J. Am. Chem. Soc.* **1993**, *115*, 11264−11269. (b) Bourdillon, C.; Demaille, C.; Moiroux, J.; Savéant, J.-M. *J. Am. Chem. Soc.* **1994**, *116*, 10328−10329. (c) Bourdillon, C.; Demaille, C.; Moiroux, J.; Savéant, J.-M. *J. Am. Chem. Soc.* **1995**, *117*, 11499−11506. (d) Bourdillon, C.; Demaille, C.; Moiroux, J.; Savéant, J.-M. *Acc. Chem. Res.* **1996**, *29*, 529−535. (e) Anicet, N.; Anne, A.; Moiroux, J.; Savéant, J.-M. *J. Am. Chem. Soc.* **1998**, *120*, 7115−7116. (f) Demaille, C.; Moiroux, J.; Savéant, J.-M.; Bourdillon, C. Antigen−antibody assembling of enzyme monomolecular layers and multimonolayers on electrodes. In *Protein Architecture: Interfacing molecular assemblies and immobilization biotechnology*; Möhwald, H., Lvov, Y., Eds.; Marcel Dekker: New York, 1999; pp 311−335.

(8) Hermanson, G. T. *Bioconjugate Techniques*; Academic Press: San Diego, 1996; p. 293.

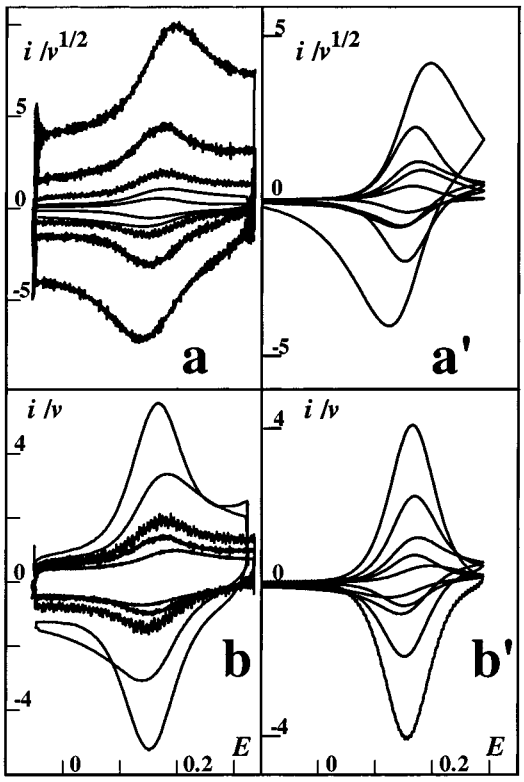

Figure 2. Potential scan rate (υ) dependence of the cyclic voltammograms. Experimental curves in a and b, simulated curves in a′ and b′, potential E in V vs SCE. The protein self-assembly contains $N = 6$ IgG−PEG−Fc monolayers, two successive IgG−PEG−Fc monolayers being separated by two monolayers of whole IgG's ($n_i = 2$). The potential scan rates are $\upsilon = 0.01$, 0.1, 1, 10, and 100 V/s. In a and a′, the current (i/μA) is normalized versus $\upsilon^{1/2}$ and the normalized signal increases with increasing υ. In b and b′, the current is normalized versus υ and the normalized signal decreases with increasing υ. Electrode surface geometric area $S = 0.07$ cm^2. Fc surface concentration in an IgG−PEG−Fc monolayer $\Gamma = 10^{-11}$ mol/cm^2. Composition of the background solution: pH 8 phosphate buffer of 0.1 M ionic strength. Temperature = 25 °C. The simulated curves in a′ and b′ do not include the background current; they were computed taking the following set of parameters: $L_{IgG}(k_{spr})^{1/2} = 85$ (J/mol)$^{1/2}$, $L_{IgG}/D^{1/2} = 8 \times 10^{-3}$ s$^{1/2}$, $L_{fs} = 22.5$ nm, $L_{IgG} = 10$ nm, and $k_e = 3.35 \times 10^9$ mol^{-1} cm^3 s^{-1} (see text).

structures which are capable of molecular recognition, namely their Fab subunits, are necessarily oriented toward the electrode.

Cyclic Voltammetry of the Wired Self-Assembly of Proteins. Determination, at Low Enough Potential Scan Rate, of the Fc Coverage in Each Immobilized IgG−PEG−Fc Molecular Monolayer. The cyclic voltammograms exhibit a very strong dependence on the potential scan rate (υ). A typical behavior is reported in Figure 2, the currents being normalized versus $\upsilon^{1/2}$ or υ in Figure 2a or b, respectively.

At sufficiently slow potential scan rates, symmetric anodic and cathodic peaks corresponding to the oxidation of the Fc heads or the reduction of the Fc^+ heads are obtained. Then the peak heights are proportional to υ, the peak-to-peak separation is less than 5 mV, and the width of each peak at mid-peak height is ca. 95 mV. Under such conditions, the Fc/Fc^+ redox couple behaves as a Nernstian redox couple for which both the reduced and oxidized forms are confined near the electrode surface.[9] That means that the variation of the electrode potential is slow enough to ensure that electron transfers between all of the Fc and Fc^+ heads present in the protein assembly and between the electrode and those which can reach the electrode proceed at equilibrium and that the mobility of the PEG chains is not rate-controlling. The ratio of the volume concentrations of Fc and Fc^+ within the whole system is controlled solely by the electrode potential. The apparent redox potential of the Fc/Fc^+ couple is given by the peak potentials.[9] The measured value of 155 ± 3 mV is in good agreement with the value of 149 ± 3 mV determined earlier with soluble PEG−Fc chains.[10] The total amount of Fc heads linked to the protein assembly is given by the area under the anodic (or cathodic) peak of the cyclic voltammogram. It was determined after each immobilization of a new IgG−PEG−Fc monolayer. Related to the geometric area of the disk electrode, an identical PEG−Fc surface concentration at saturation (Γ) was found in each IgG−PEG−Fc monolayer, as expected for the self-assembly of a molecular monolayer whose surface density is controlled, at saturation coverage, solely by maximum lateral compactness.[1,7] We used two different batches of IgG−PEG−Fc bioconjugates and found Γ to be either $(1.0 \pm 0.1) \times 10^{-11}$ mol/cm^2 or $(1.4 \pm 0.1) \times 10^{-11}$ mol/cm^2. Such values correspond to IgG surface concentrations in IgG−PEG−Fc monolayers of ca. 0.8×10^{-12} mol/cm^2. The IgG surface concentration in the spacer monolayers is certainly greater, probably ca. 2.7×10^{-12} mol/cm^2 as demonstrated in previous works.[7] The lesser coverage obtained with the IgG bearing ca. 17 PEG−Fc chains is a consequence of the greater bulkiness of IgG−PEG−Fc due to the attachment of the PEG−Fc chains. The molar weight of the PEG chains is 3400 g/mol on average and they probably take coil conformations of end-to-end length equal to the corresponding Flory radius (R_F) of ca. 5 nm.[11] The ensuing contribution to IgG−PEG−Fc bulkiness is thus considerable since the IgG size lies in the 10−15 nm range.[12] The irreversibility of the binding is ascertained by the persistence of the electrochemically assayed ferrocene coverage. Less than 10% is lost in 4 weeks.

The outstanding regularity of the spatial distribution and of the reproducibility of the IgG coverage obtained in each molecular monolayer immobilized by the use of the immunological step-by-step construction has been well established and documented in a series of previous reports.[7] First of all, molecular monolayers of glucose oxidase-labeled antibodies (glucose oxidase−antibody conjugates) were successively self-assembled at the electrode surface, and the resulting catalytic activity was measured in the presence of glucose and ferrocene methanol, a redox mediator, diffusing freely through the immobilized protein assembly. It was then shown that the same amount of glucose oxidase−antibody conjugate was immobilized in each step.[7b] The measurement of the catalytic activity also indicated that the surface concentration of immobilized enzyme in each monolayer corresponded to a molecular monolayer of maximal lateral compactness.[7b,c] Quantitative analysis of the kinetic competition between the rate of diffusion of the redox mediator and the rate of its consumption by the enzyme-catalyzed reaction gave access to the spatial distribution of the monolayers of enzyme active sites.[7c] Particularly the distance separating the electrode surface from the first monolayer of immobilized active enzyme was varied by inactivation of various numbers of already immobilized monolayers of enzyme−antibody conjugates before attachment of a new monolayer of

(9) Laviron, E. *Voltammetric Methods for the Study of Adsorbed Species. In Electroanalytical Chemistry*; Bard, A. J., Ed.; Marcel Dekker: New York, 1982; Vol. 12, pp 53−157.

(10) Demaille, C.; Moiroux, J. *J. Phys. Chem. B* **1999**, *103*, 9903−9909.

(11) Vincent, B.; Luckham, P.; Waite, F. A. *J. Colloid Interface Sci.* **1980**, *73*, 508−521.

(12) Lamy, J.; Lamy J.; Billiald, P.; Sizaret, P. Y.; Cavé, G.; Frank, J.; Motta, G. *Biochemistry* **1985**, *24*, 5532−5542.

active enzymes. The distance separating two successively immobilized monolayers of enzyme−antibody conjugates appeared quite reproducible within the whole structure of proteins self-assembled according to the step-by-step procedure.[7c] The regularity of the spatial distribution thus obtained shows that the driving force of immunological recognition is strong enough to make it prevail over equilibriums of lower driving forces such as nonspecific binding and aggregate formation. Therefore, the remarkable reproducibility obtained for the Fc coverage in the IgG−PEG−Fc molecular monolayers which were successively immobilized by means of the same immunological step-by-step construction is not surprising. Figure 1 is a schematic sketch, the three linked lobes of which a whole IgG is made, may not be displayed as linearly as drawn in the figure for the sake of clarity; however, they surely arrange so as to ensure a reproducible distance between two successive molecular monolayers of immobilized IgG's of maximum lateral compactness. The antigen−antibody systems, which are used for the construction, are polyclonal. Moreover, they are capable of whole IgG recognition with no specificity toward any particular site of the IgG, not even the γ chain. The different clones can have different surface charge densities; however, the ionic strength of the surrounding buffer is high enough to neutralize the effect of local electrostatic repulsion, or attraction, that those charge densities could cause at low ionic strength.[13] As underlined in earlier reports,[7] the reproducibility of the IgG coverage in each molecular monolayer results precisely from the polyclonal character of the immunological species which self-assemble in order to ensure maximum lateral compactness of each successively immobilized monolayer. When there remains an empty space which is large enough to allow the attachment of a molecule of antibody, there always exists, in the pool of polyclonal antibodies contained in the solution used for the immobilization step, an antibody which is able to recognize the antigen in the underlying monolayer and thus fill the empty space.

Effect of Increasing Potential Scan Rate. The range of potential scan rates giving rise to symmetric anodic and cathodic peaks with heights proportional to v depends on N, the total number of IgG−PEG−Fc monolayers, and n_i the number of IgG spacers introduced between two successive IgG−PEG−Fc monolayers. The larger N or n_i, the smaller the scan rates, giving rise to symmetric anodic and cathodic peaks. The effect of N is obvious in Figures 3 and 4 which provides also clear evidence of the effect of n_i.

When the potential scan rate is not slow enough to allow the whole system of electron transport to proceed at equilibrium, the peaks in the cyclic voltammogram are drawn out. As can be seen in Figures 3 and 4, the anodic peak current (i_{pa}) increases less than expected from a proportionality to v and more than expected from a proportionality to $v^{1/2}$. The most striking feature of the data reported in Figures 3 and 4 is the nonuniform dependence of the anodic (E_{pa}) and cathodic (E_{pc}) peak potentials on v that are observed as soon as $N \geq 2$. The peak potentials remain practically symmetric to the standard potential (E^0_{PQ}) of the Fc/Fc^+ redox couple. However, the peak-to-peak separation ($\Delta E_p = E_{pa} - E_{pc}$) increases in a first range of increasing v, then levels or even decreases, and increases again with increasing v as can be seen in Figures 3 and 4.

For $v \geq 50$ V/s, E_{pa}, E_{pc}, and i_{pa} become N- and n_i-independent, and the voltammograms are identical with those recorded and analyzed in a previous work when only one IgG−PEG−Fc monolayer was immobilized at various distances away from the electrode surface.[1] That means that, at sufficiently high potential scan rates ($v \geq 50$ V/s), the sole type of electron transfer which is kinetically allowed to take place is the heterogeneous electron transfer between the electrode surface and the ferrocene heads attached to the first IgG−PEG−Fc monolayer. It was shown that, under such conditions, the heterogeneous electron transfer is Nernstian and the recorded current is a measure of the dynamics of the PEG chains.[1]

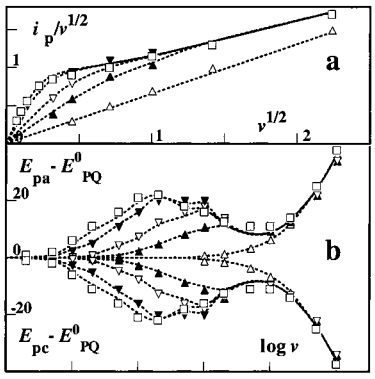

Figure 3. Dependence of anodic peak current (i_p/μA), anodic (E_{pa}/mV), and cathodic (E_{pc}/mV) peak potentials on the potential scan rate (v in V/s) in cyclic voltammetry for wired self-assemblies containing various numbers (N) of IgG−PEG−Fc monolayers, two successive IgG−PEG−Fc monolayers being separated by $n_i = 2$ monolayers of whole IgG's. $N = 1$ (△), 2 (▲), 3 (▽), 5 (▼), or 6 (□). Same experimental conditions as in Figure 2. The simulated values (dotted curves) are computed using the same set of parameters as in Figure 2.

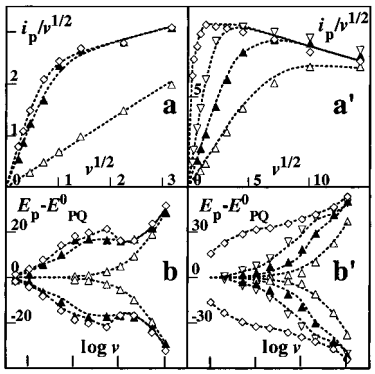

Figure 4. Dependence of anodic peak current (i_p/μA), anodic (E_{pa}/mV), and cathodic (E_{pc}/mV) peak potentials on the potential scan rate (v in V/s) in cyclic voltammetry for wired self-assemblies containing various numbers (N) of IgG−PEG−Fc monolayers. In a and b, two successive IgG−PEG−Fc monolayers are separated by $n_i = 1.5$ spacers; in a′ and b′ they are separated by $n_i = 1$ spacer. In a and b, $N = 1$ (△), 5 (▲), or 5 (◇). In a′ and b′, $N = 1$ (△), 2 (▲), 4 (▽), or 19 (◇). Same experimental conditions as in Figure 2, except that $\Gamma = 1.6 \times 10^{-11}$ mol/cm^2 in a′ and b′. The simulated values (dotted curves) are computed using the same set of parameters as in Figure 2.

Quantitative Analysis of the Dynamics of Electron Transport within the Wired Self-Assembly of Proteins. We are interested only in the efficiency of electron transport perpendicularly to the electrode surface, and we will consequently restrict the formulation of the quantitative analysis of the dynamics of the system to this sole dimension. The parameters we define in the following reflect the net contribution of the processes we consider along the sole direction perpendicular to the electrode surface.

As already mentioned, the dynamics of the PEG chains can be thoroughly and quantitatively characterized when only one IgG−PEG−Fc monolayer is immobilized at the electrode

(13) Feinberg, B. A.; Ryan, M. D. *J. Inorg. Biochem.* **1981**, *15*, 187−199.

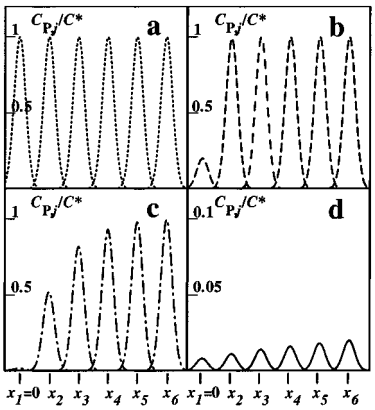

Figure 5. Concentration profiles of P_j heads at the end of the forward potential scan in cyclic voltammetry depending on potential scan rate (υ). Same wired protein assembly and same experimental conditions as in Figure 3. The volume concentration of P_j ($C_{P,j}$) is normalized versus C^* (see text). The simulated profiles are computed using the same set of parameters as in Figure 3. (a) spatial distribution at the initial potential. (b) $\upsilon = 100$ V/s. (c) $\upsilon = 1$ V/s. (d) $\upsilon = 0.01$ V/s, note that the scale on y axis is expanded by a factor of 10 in this case. The distance $x_{j+1} - x_j$ ($j \geq 1$) is 30 nm.

surface and a model of elastic bounded diffusion justifying satisfactorily the experimental results was elaborated.[1] According to this model of elastic bounded diffusion, the time (t) and space (x) dependence of the volume concentration of ferrocene heads is given by a modified form of the second Fick law, the reduced ferrocene form being noted P in the following:[1]

$$\frac{\partial C_P}{\partial t} = D\left[\left(\frac{\partial^2 C_P}{\partial x^2}\right) + \left(\frac{k_{spr}D}{RT}\right)\left(\frac{\partial C_P}{\partial x}\right)\right] \quad (1)$$

in which C_P is the P volume concentration, D the diffusion coefficient of the ferrocene head defined by the Einstein relation ($D = k_BT/k_{dr}$ with k_{dr} the corresponding drag coefficient and k_B the Boltzmann constant), k_{spr} the spring constant of the PEG chain mimicked by an harmonic oscillator and x the spring elongation away from the resting position of the ferrocene head. Similarly the Fc^+ (noted Q in the following) volume concentration (C_Q) dependence on t and x is given by an equation analogous to eq 1. The dynamics of a PEG chain does not depend on whether it bears a P or a Q head; thus, D and k_{spr} are identical for P and Q, and whatever t and x:

$$C_P^0 = C_P + C_Q \quad (2)$$

C_P^0 being the initial volume concentration given by the spatial distribution of ferrocene heads when the wired protein assembly exists in its fully reduced form. The average position at which the PEG−Fc chains of the jth IgG−PEG−Fc monolayer are terminally attached is x_j ($1 \leq j \leq N$). Statistically x_j corresponds to the position of the center of the IgG part of IgG−PEG−Fc when the immunoglobulin is assimilated to a sphere. Algebraically, x_1 is taken as zero, meaning that the electrode surface is located at $-x_{el}$ as shown in Figure 5. Then the initial profile of the volume concentration of ferrocene heads attached to the jth IgG−PEG−Fc monolayer ($C_{P,j}^0$) along the x axis is given by a Gaussian distribution:

$$C_{P,j}^0 = C^* \exp\left[\frac{-k_{spr}(x - x_j)^2}{2RT}\right] \quad \text{with} \quad C^* = \Gamma\left(\frac{k_{spr}}{2\pi RT}\right)^{1/2}$$

[1,14] since Γ is the same for each IgG−PEG−Fc monolayer. The initial spatial distribution of $C_{P,j}^0$ is reproduced in Figure 5a.

Taking L_{IgG} as the statistically averaged size of a whole IgG spacer, $L_{IgG}/2$ for a Fab fragment, x_j is then $x_j = (j-1)(n_i+1)L_{IgG}$ for $j > 1$, the distance separating two successive IgG−PEG−Fc monolayers is $(n_i+1)L_{IgG}$ and $x_{el} = 1.5L_{IgG}$ according to the construction sketched in Figure 1. The ferrocene heads of the first IgG−PEG−Fc monolayer can reach the electrode surface only when $1.5L_{IgG} < L_{fs}$, L_{fs} being the length of the fully stretched PEG chain. Contact between the ferrocene heads of two successive IgG−PEG−Fc monolayers cannot occur when $0.5(n_i+1)L_{IgG} > L_{fs}$.

The kinetic contribution of isotopic electron transfer between P and Q heads pertaining to successive IgG−PEG−Fc monolayers along the x axis is $V_e = k_e(C_{Q,j}C_{P,j+1} - C_{P,j}C_{Q,j+1})$ at any t and x, k_e being the corresponding rate constant, provided that $x_{j+1} - L_{fs} \leq x \leq x_j + L_{fs}$, that is that contact between the ferrocene heads of two successive IgG−PEG−Fc monolayers is a priori possible. Taking eq 2 into account, that gives:

$$\frac{\partial C_{P,j}}{\partial t} = k_e[C_{P,j}^0 C_{P,j+1} - C_{P,j+1}^0 C_{P,j}] \quad (3)$$

The heterogeneous electron transfer occurring at the electrode surface is rapid compared to the chain mobility;[1] thus, the ratio $C_{P,-xel}/C_{Q,-xel}$ is related to the electrode potential E by the Nernst law:

$$\frac{C_{P,-xel}}{C_{Q,-xel}} = \exp\left[-\left(\frac{F}{RT}\right)(E - E_{PQ}^0)\right] \quad (4)$$

The following changes in variables and parameters lead to a dimensionless formulation of the problem.

$$\tau = \left(\frac{F\upsilon}{RT}\right)t;\ y = x\left(\frac{F\upsilon}{RTD}\right)^{1/2};\ \mu = x_{el}\left(\frac{F\upsilon}{RTD}\right)^{1/2};\ l = L_{fs}\left(\frac{F\upsilon}{RTD}\right)^{1/2}$$

$$\epsilon = (n_i+1)L_{IgG}\left(\frac{F\upsilon}{RTD}\right)^{1/2};\quad p_j = \frac{C_{P,j}}{C^*};\quad q_j = \frac{C_{Q,j}}{C^*};$$

$$\lambda = \left(\frac{RT}{F\upsilon}\right)k_eC^*;\quad \xi = \left(\frac{F}{RT}\right)(E - E_{PQ}^0)$$

The Nernst eq 4 becomes:

$$p_{-xel} = q_{-xel}\exp(-\xi) \quad (4')$$

The dimensionless current ψ is $\psi = i/[(FS\Gamma/RT)(2FDk_{spr}\upsilon/\pi)^{1/2}]$, i being the actual current, and S is the electrode surface geometric area. The dimensionless parameter $\beta = k_{spr}D/F\upsilon$ compares the experimental observation time $RT/F\upsilon$ to the characteristic chain motion time $RT/k_{spr}D$.[1]

The set of partial differential equations describing the dynamics of the P heads, when electron transfer can proceed between two successive IgG−PEG−Fc monolayers, is:

$$\text{for } -\mu \leq y < \epsilon - l:\quad \frac{\partial p_1}{\partial \tau} = \frac{\partial^2 p_1}{\partial y^2} + \beta p_1 + \frac{\beta y \partial p_1}{\partial y}$$

for $(j-2)\epsilon + l < y < j\epsilon - l$ (with $1 < j \leq N$):

$$\frac{\partial p_j}{\partial \tau} = \frac{\partial^2 p_j}{\partial y^2} + \beta p_j + \beta[y - (j-1)\epsilon]\frac{\partial p_j}{\partial y}$$

(14) Rigorously, $C^* = \Gamma(k_{spr}/2\pi RT)^{1/2}/\text{erf}[L_{fs}(k_{spr}/2RT)^{1/2}]$.[1] However $\text{erf}[L_{fs}(k_{spr}/2RT)^{1/2}] = 1$ with less than 1% error in the present circumstances.

for $j\epsilon - l \le y \le (j-1)\epsilon + l$ (with $1 \le j < N$):

$$\frac{\partial p_j}{\partial \tau} = \frac{\partial^2 p_j}{\partial y^2} + \beta p_j + \beta[y-(j-1)\epsilon]\frac{\partial p_j}{\partial y} + \lambda\{p_{j+1}\exp(-0.5\beta[y-(j-1)\epsilon]^2) - p_j\exp(-0.5\beta[y-j\epsilon]^2)\}$$

$$\frac{\partial p_{j+1}}{\partial \tau} = \frac{\partial^2 p_{j+1}}{\partial y^2} + \beta p_{j+1} + \beta(y-j\epsilon)\partial p_{j+1}/\partial y + \lambda\{p_j\exp(-0.5\beta[y-j\epsilon]^2) - p_{j+1}\exp(-0.5\beta[y-(j-1)\epsilon]^2)\}$$

for $y > (N-2)\epsilon + l$:

$$\frac{\partial p_N}{\partial \tau} = \frac{\partial^2 p_N}{\partial y^2} + \beta p_N + \beta[y-(N-1)\epsilon]\frac{\partial p_N}{\partial y}$$

The dynamics of the Q heads can be described by a similar set of partial differential equations. However p_j and q_j being related by eq 4′ at $y = -\mu$ whatever τ and j, and by $p_j + q_j = \exp(-0.5\beta[y-(j-1)\epsilon]^2)$ whatever y, τ, and j, only one set of partial differential equations need be solved.

The initial and boundary conditions are:

$\tau = 0, y \ge -\mu, 1 \le j \le N$:

$$p_j = \exp\{-0.5\beta[y-(j-1)\epsilon]^2\}, \qquad q_j = 0$$

$\tau \ge 0, y = -\mu$

$$p_{1,-\mu} = \exp(-0.5\beta\mu^2)\exp(-\xi)/[1+\exp(-\xi)]$$

$$\psi = [(\partial p_1/\partial y)_{-\mu} - \beta\mu p_{1,-\mu}]/2$$

$\tau \ge 0, y = (j-1)\epsilon - l$ (with $1 < j \le N$):

$$\left(\frac{\partial p_j}{\partial y}\right) - \beta l p_j = \lambda dy\{p_{j-1}\exp(-0.5\beta l^2) - p_j\exp[-0.5\beta(l-\epsilon)^2]\}$$

$\tau \ge 0, y = (j-1)\epsilon + l$ (with $1 \le j < N$):

$$\left(\frac{\partial p_j}{\partial y}\right) + \frac{\beta}{p_j} = \lambda dy\{p_{j+1}\exp(-0.5\beta l^2) - p_j\exp[-0.5\beta(l-\epsilon)^2]\}$$

$\tau \ge 0, y = (N-1)\epsilon + l$: $\qquad \dfrac{\partial p_N}{\partial y} + \dfrac{\beta}{p_N} = 0$

The set of differential equations can be solved numerically as described in Supporting Information. Computations allow the simulation of cyclic voltammogram for any set of the parameters β, λ, l, μ, and ϵ. The last two parameters being related, since $\mu/\epsilon = 1.5/(n_i + 1)$, the simulated voltammograms depend on four independent parameters, namely β, λ, l, and either μ or ϵ. However, it was established previously[1] that for such a protein assembly containing an IgG−PEG−Fc monolayer $A = L_{IgG}(k_{spr})^{1/2} = (93 \pm 10)$ (J/mol)$^{1/2}$ and $B = L_{IgG}/D^{1/2} = (7 \pm 2) \times 10^{-3}$ s$^{1/2}$; therefore, β and μ (hence ϵ) are known since $\beta = A^2/F\upsilon B^2$ and $\mu = 1.5(F\upsilon/RT)^{1/2}B$. The length of the fully stretched PEG chain L_{fs} can be deduced from molecular models, and L_{IgG} can also be deduced from the IgG images reproduced in ref 12. That gives l since $l = (L_{fs}/L_{IgG})(F\upsilon/RT)^{1/2}B$. Thus, in the present study, λ is the sole dimensionless parameter we have to adjust. At a given potential scan rate υ, λ depends only on the rate constant of isotopic electron exchange k_e since $\lambda = (RT/F\upsilon)k_eC^* = k_e(RT/F\upsilon)(\Gamma A/L_{IgG})(1/2\pi RT)^{1/2}$.

The numerical computations were carried out using the following set of values: $L_{IgG}(k_{spr})^{1/2} = 85$ (J/mol)$^{1/2}$, $L_{IgG}/D^{1/2} = 8 \times 10^{-3}$ s$^{1/2}$, $L_{fs} = 22.5$ nm and $L_{IgG} = 10$ nm. Then the best fit with the experimental data was obtained for $k_e = 3.35 \times 10^9$ mol^{-1} cm^3 s^{-1}. The simulated cyclic voltammograms reproduced in Figure 2 exhibit the same characteristic features as the experimental ones once it is taken into account that the experimental signals contain a background current which is mainly capacitive, proportional to υ, and not added to the simulated curves. More explicitly the original dependence of the peak potentials and of the anodic peak current on υ is quite satisfactorily justified as can be seen in Figures 3 and 4. When $(n_i + 1)\,L_{IgG} < L_{fs}$ as is the case when $n_i = 1$, Q_j can react with both P_{j+1} and P_{j+2} and conversely P_j with Q_{j+1} and Q_{j+2}. That means that new kinetic terms must be included in the boundary conditions and in the partial differential equations, for the concerned y intervals, thus rendering the equations more cumbersome although not intractable (see Supporting Information).

The Pj volume concentration profiles computed at the end of the forward potential scan are reported in Figure 5. In Figure 5b they show that, at sufficiently high potential scan rate, only the ferrocene heads of the first IgG−PEG−Fc monolayer are oxidized within the time window of the measurement, whereas on the other hand, at sufficiently low potential scan rate practically all of the ferrocene heads attached to the protein assembly are oxidized at the end of the forward potential scan (Figure 5d). The P_j concentration profiles also give a clear image of the space regions where the profiles of P_j and P_{j+1} overlap and where isotopic electron transfer between P and Q heads linked to successive IgG−PEG−Fc monolayers can take place and ensure electron transport. The larger the overlap, the greater the rate of electron transport. Once the PEG chain and the IgG species are chosen, the width of overlap is controlled by n_i, and Figures 3 and 4 provide quantitative evidence of the influence of n_i.

At a given abscissa x, the greater $C_{Q,j}$ (i.e., smaller $C_{P,j}$) and $C_{P,j+1}$, the faster the electron transport for oxidation, and conversely for reduction. It must be emphasized that the maximum values of $C_{Q,j}$ and $C_{P,j+1}$ are given by the initial concentration profiles (Figure 5a) which depend essentially on the PEG chain stiffness through the spring constant k_{spr}. For the PEG chains of 3400 g molar weight on average, the ferrocene head volume concentration becomes practically zero in the space regions where the required elongation would exceed 1.5 L_{IgG}. The simulations also confirm that the peak potentials and the peak currents are quite sensitive to the rate constant of isotopic electron exchange as soon as the electron transport extends beyond the first IgG−PEG−Fc monolayer; over the whole set of experiments we carried out, we found that $3.0 \times 10^9 \le k_e \le 3.6 \times 10^9$ mol^{-1} cm^3 s^{-1}.

Actually, the ferrocene heads of the first IgG−PEG−Fc monolayer act as a redox catalyst[15] for the oxidation of the ferrocene heads of the following IgG−PEG−Fc monolayer and so on. Eventually, the amplitude of propagation of the electron transport along the x axis depends on υ. The first limiting

(15) (a) Savéant, J.-M.; Vianello, E. In *Advances in Polarography*; Longmuir, E. S., Ed., Pergamon Press: London, 1960; Vol. 1, pp 367−374. (b) Andrieux, C. P.; Savéant, J.-M. Electrochemical reactions. In *Investigations of Rates and Mechanisms of Reactions, Techniques in Chemistry*; Bernasconi, C., Ed.; Wiley: New York, 1986; Vol. 6, 4/E, Part 2, pp 305−390.

situation is reached at υ slow enough to allow total redox catalysis. Then all of the ferrocene heads behave as if they were confined to the electrode surface, consequently $\Delta E_p \rightarrow 0$ and i_{pa} is proportional to υ.[9] When leaving the first limiting situation by increasing υ, the redox catalysis ceases being total. A catalytic-like contribution to the signal is still obtained as long as the P heads of the first IgG−PEG−Fc monolayer are exhaustively oxidized during the course of the forward potential scan. The catalytic-like contribution is then controlled by $\lambda = (RT/F\upsilon)k_eC^*$, the efficiency of the redox catalysis decreases with increasing υ, and i_{pa} is less and less than expected, according to proportionality to υ. In a first interval of υ, when the redox catalysis is still efficient, ΔE_p increases with increasing υ.[15a] In a second interval of υ, the efficiency of the redox-like catalysis becomes very small, and the cyclic voltammogram tends to reflect the sole dynamics of the PEG−Fc chains of the first IgG−PEG−Fc monolayer. Then ΔE_p decreases and tends toward the value observed at the same potential scan rate in the presence of only one IgG−PEG−Fc monolayer.[1] The last limiting situation, which is reached at high υ, corresponds to pure kinetic control by PEG chain stiffness. Then ΔE_p increases monotonically with increasing υ and i_{pa} tends to become proportional to $\upsilon^{1/2}$ as previously reported.[1]

As stated earlier, the best fit between the computed and experimental data was achieved in the present quantitative study by considering that $L_{IgG}(k_{spr})^{1/2}$, $L_{IgG}/D^{1/2}$, L_{fs}, and L_{IgG} were known and by taking k_e as the sole adjustable parameter. The value we obtained for k_e must then be compared to the conventional volume rate constant $k_{e,s}$ of isotopic electron transfer between ferrocene and ferrocenium derivatives in solution which can be found in the literature.[16] The protein self-assembly proceeds with low compactness and the solvent−solute interactions within the assembly do not differ from those in solution.[7,10] Therefore, k_e should be $k_{e,s}/6$, the factor 1/6 being introduced because in a three-dimension bulk solution, reactions may occur along the two directions of the three space coordinates, while here electron transfers occurring along the two coordinates defining a plane parallel to the electrode surface or along the positive direction of the x coordinate do not contribute to the flux we calculate.[4f,5] For ferrocene methanol in water,[16] $k_{e,s}$ is 1.4×10^{10} mol^{-1} cm^3 s^{-1} and thus $k_e = 2.3 \times 10^9$ mol^{-1} cm^3 s^{-1}. The value $k_e = (3.3 \pm 0.3) \times 10^9$ mol^{-1} cm^3 s^{-1} is obviously in coherence with the kinetics of electron self-exchange between ferrocene and ferrocenium derivatives, and the pertinence of the model we elaborated for quantitative analysis of the kinetic behavior of the wired protein assembly is thus strongly supported.

Wiring of a Redox Enzyme Immobilized on Top of the Protein Self-Assembly. As already mentioned, immobilization of an enzyme molecular monolayer on top of the *N*th IgG−PEG−Fc monolayer was achieved by immunological reaction with a glucose oxidase IgG conjugate.[7] That the glucose oxidase enzyme is wired is ascertained by the catalytic currents recorded in the presence of glucose as shown in Figure 6.

If, in addition to glucose, ferrocene methanol is added to the solution, the catalytic response obtained in cyclic voltammetry is more than 10 times greater. The contribution of the mediation by ferrocenium attached to the protein assembly to the catalytic current is then actually negligible compared to that of the mediation by the solution ferrocene methanol (0.4 mM), and the amount of immobilized active enzyme may be derived from the catalytic current obtained under these conditions.[7] In the series of experiments we carried out, the enzyme surface concentration (Γ_E), related to the geometric area, was found to lie in the 0.9 to 1.1 $\times$ 10^{-12} mol/cm^2 range. That is roughly half the surface concentration obtained when the enzyme−antibody conjugate reacted with an immobilized underlying monolayer of immunoglobulin bearing no PEG−Fc chains.[7] The smaller enzyme coverage results from the decrease in IgG surface concentration within the *N*th IgG−PEG−Fc monolayer which is caused, as already pointed out, by the bulkiness of the PEG coils. The homemade purified enzyme−antibody conjugate that we used has a stoichiometry of one glucose oxidase per IgG (see the Experimental Section). Consequently Γ_E cannot be much greater than the IgG surface concentration within the *N*th IgG−PEG−Fc monolayer (ca. 0.8×10^{-12} mol/cm^2), the difference between the two surface concentrations being due to the fact that some IgG molecules can undergo multiple recognition when the steric constraints are not forbidding. When the enzyme surface concentration is controlled by maximum lateral compactness of the enzyme monolayer, Γ_E is ca. 2.6×10^{-12} mol/cm^2. Therefore, when Γ_E is ca. 0.8×10^{-12} mol/cm^2, the enzyme−antibody conjugate may lay flat on the *N*th IgG−PEG−Fc monolayer as indicated in Figure 1d, and the center of the glucose oxidase moiety is, on statistical average, located at $x_E = x_N + L_{IgG}$, the size of glucose oxidase, assimilated to a sphere, being the same as the IgG size.[7] In the following we will assume that the profile of the enzyme active-sites' volume concentration (C_E) along the x axis corresponds to a Gaussian distribution extending over the $x_N + 0.5L_{IgG}$ to $x_N + 1.5L_{IgG}$ interval and centered at x_E. Then $C_E = C_E^* \exp\{-a_E[(x - x_E)/L_{IgG}]^2\}$ with $C_E/C_E^* = 0.01$ for $|x - x_E| = 0.5L_{IgG}$; hence, $a_E = 18.4$ and $C_E^* = (\Gamma_E/L_{IgG})\sqrt{18.4/\pi}$. In the present case, all of the enzyme active sites can be reached

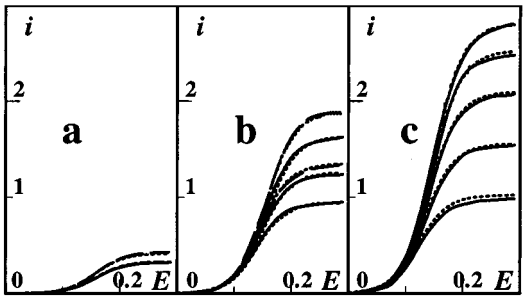

Figure 6. Catalytic currents (i/μA) obtained with a molecular monolayer of glucose oxidase immobilized on top of a wired self-assembly of proteins, depending on the number of IgG−PEG−Fc monolayers (N) and the number of spacers (n_i) separating two successive IgG−PEG−Fc monolayers. Potential E in V vs SCE, potential scan rate $\upsilon = 0.005$ V/s, the current responses are υ independent, provided that $\upsilon \leq 0.010$ V/s. (a) $n_i = 2$, the superimposed continuous curves give the catalytic responses for $N = 5$ and glucose concentrations C_G^0 of 10 and 160 mM, the superimposed dashed curves give the catalytic responses for $N = 4$ and same glucose concentrations. (b) $n_i = 1.5$, the continuous curves give the catalytic responses for $N = 5$ and glucose concentrations C_G^0 of 10, 20 and 160 mM, the dashed curves give the catalytic responses for $N = 4$ and same glucose concentrations, for the lowest glucose concentration (10 mM) the current responses for $N = 4$ and $N = 5$ are superimposed. (c) $n_i = 1$ and $N = 4$ the continuous curves were obtained with $C_G^0 = 10$, 20, 40, 80, and 160 mM respectively. Same experimental conditions as in Figure 2, enzyme surface concentration $\Gamma_E = 10^{-12}$ mol/cm^2. The simulated (dotted) curves are computed taking the same sets of parameters as in figures 2−4 and $k_3 = 2.5 \times 10^8$ mol^{-1} cm^3 s^{-1}, $k_2 = 700$ s^{-1}, and $k_{red} = 10^7$ mol^{-1} cm^3 s^{-1}, the spatial distribution of enzyme active sites being as discussed in the text.

(16) (a) Nielson, R. M.; McManis, G. E.; Weaver, M. J. *J. Phys. Chem.* **1989**, *93*, 4703−4706. (b) McManis, G. E.; Nielson, R. M.; Gochev, A.; Weaver, M. J. *J. Am. Chem. Soc.* **1989**, *111*, 5533−5541.

by the ferrocene heads of the *N*th IgG−PEG−Fc monolayer since $1.5L_{IgG} < L_{fs}$.

The origin of the catalytic current measured in the presence of glucose is the regeneration of P_N by reduction of the oxidized form Q_N of the ferrocene heads which can reach enzyme active sites according to the well-known mechanism of enzyme catalysis by glucose oxidase[7a−c,18,19]

$$\mathrm{FAD} + \mathrm{G} \underset{k_{-1}}{\overset{k_1}{\rightleftharpoons}} \mathrm{FADG}$$

$$\mathrm{FADG} \xrightarrow{k_2} \mathrm{FADH_2} + \mathrm{Gl}$$

$$\mathrm{FADH_2} + 2\,\mathrm{Q} \xrightarrow{k_3} \mathrm{FAD} + 2\,\mathrm{P}$$

with FAD = oxidized flavin of the glucose oxidase flavoprotein, G = glucose, FADG = enzyme−substrate precursor complex, $FADH_2$ = reduced flavin, Gl = glucono-δ-lactone.

That gives for the rate of P_N regeneration at a given abscissa:[7]

$$\frac{\partial p_N}{\partial \tau} = \lambda_E e\{\exp(-0.5\beta[y-(N-1)\epsilon]^2) - p_N\}/ \{1+\sigma[\exp(-0.5\beta[y-(N-1)\epsilon]^2)] - p_N\}$$

in dimensionless formulation with $\lambda_E = 2k_3C_E^*(RT/F\upsilon)$, $e = C_E/C_E^*$, $\sigma = k_3C_E^*(1/k_2 + 1/k_{red}C_G^0)$, $k_{red} = k_1/(k_{-1}+k_2)$, and C_G^0 = glucose bulk volume concentration (in excess).

The set of partial differential equations must then be modified as follows in the $(N-1)\epsilon + 0.5\epsilon/(n_i+1) \le y \le (N-1)\epsilon + 1.5\epsilon/(n_i+1)$ interval:

$$\frac{\partial p_N}{\partial \tau} = \frac{\partial^2 p_N}{\partial y^2} + \beta p_N + \beta[y-(N-1)\epsilon]\frac{\partial p_N}{\partial y} + \lambda_E e\{\exp(-0.5\beta[y-(N-1)\epsilon]^2) - p_N\}/ \{1+\sigma[\exp(-0.5\beta[y-(N-1)\epsilon]^2)] - p_N\}$$

For the computations of the catalytic voltammograms, the rate constants k_2 and k_{red} were taken as having their usual values at pH 8, since they are related only to the reaction between the oxidized flavin and glucose;[17] thus, $k_2 = 700\ s^{-1}$ and $k_{red} = 10^7\ mol^{-1}\ cm^3\ s^{-1}$.[18,19] Then the sole adjustable parameter was rate constant k_3.

A catalytic current is obtained only when Q heads can reach the enzyme active sites. The quantitative analysis of the dynamics of electron transport through the wired protein assembly shows that the potential scan rate υ must then not be too fast since allowance must be made for Q head production in the *N*th IgG−PEG−Fc monolayer. To ensure experimentally that electron transport proceeded at full capacity, we decreased υ down to values for which the catalytic currents were υ-independent.

When the rate of electron transport (i.e. the rate of production of Q in the *N*th IgG−PEG−Fc monolayer) through the wired assembly is slow compared to the rate of consumption of Q in the region where the enzyme-catalyzed reaction takes place, the resulting current is controlled solely by the dynamics of the wired assembly. If there exists, below enzyme substrate saturation, a glucose concentration C_G^0 high enough to bring on kinetic control by electron transport, the catalytic current becomes C_G^0 insensitive above such a critical concentration. Then the enzyme wiring is not satisfactory. As demonstrated in the quantitative analysis of the dynamics of electron transport through the wired protein assembly, the greater N and n_i, the more probable the kinetic control by electron transport, the effect of n_i being the most crucial. According to the voltammograms reproduced in Figure 6a, such a limiting situation is clearly reached for $n_i = 2$ and $N = 5$ and even 4. Figure 6b and c shows that the C_G^0 sensitivity is markedly improved when, for $N = 4$, n_i is decreased down to 1.5 and 1. The experimental data ascertain that the catalytic current is solely controlled by the enzymatically catalyzed process when $C_G^0 = 10$ mM and $n_i = 1$ or 1.5, N being 4 or 5, since identical catalytic currents are recorded (see Figure 6b and c). Simulations show that for $n_i = 1$ the catalytic current is practically N-independent until $C_G^0 = 80$ mM. For $n_i = 1.5$ (Figure 6b) the catalytic current is clearly N-dependent as soon as $C_G^0 > 10$ mM.

When the enzyme-catalyzed process contributes at least in part to the kinetic control of the integrated system, the best fit between the simulated and experimental curves gives $k_3 = (2.5 \pm 0.2) \times 10^8\ mol^{-1}\ cm^3\ s^{-1}$. This is a priori an apparent rate constant since the rate constant of reaction of the Q head of a terminally attached PEG chain with the reduced flavin buried within the enzyme may well depend on the elongation required for the PEG chain. Nevertheless, comparison with the reactivity of various ferrocenium derivatives with reduced glucose oxidase shows that $k_3 = (2.5 \pm 0.2) \times 10^8\ mol^{-1}\ cm^3\ s^{-1}$ corresponds to an efficient redox mediation.[7c,19] The rate constant k_3 for small molecules such as dioxygen or ferrocene methanol which can act as redox mediator for glucose oxidase is 10 (for dioxygen at pH 6.5)[18] to 100 (for ferrocene methanol at pH 8.0)[19] times greater. Moreover, they diffuse freely within the protein assembly and can transport electrons much more rapidly than the "wired" structure described in the present work. Therefore, the integrated system under consideration cannot compete kinetically with systems making use of freely diffusing dioxygen or ferrocene methanol; however, such systems are not integrated.

Experimental Section

Chemicals. The polyclonal antibodies, affinity-purified whole IgG molecules of ca. 150000 g/mol molar weight or Fab fragments were from Jackson laboratories and were used as received. The bioconjugate of mouse anti-goat IgG with minimal cross-reactivity to human, mouse and rabbit serum proteins bearing covalently and terminally attached ferrocene end-labeled poly(ethylene glycol) linear chains (IgG−PEG−Fc) was synthesized as described earlier.[1] The glucose oxidase conjugate of goat anti-mouse IgG was synthesized following classical procedures[8] and purified so as to ensure that the stoichiometry of the reagent we used was one glucose oxidase per one IgG.[20]

Step-by-Step Construction of the IgG Multilayer Assembly. The 3 mm diameter glassy carbon disk electrodes were prepared as described previously.[19a] They were successively polished with sand paper and diamond pastes of 3 and 1 μm particle size. The electrodes were ultrasonicated in dichloromethane between each polishing step. The adsorbed monolayer of IgG produced in goat and the first IgG−PEG−Fc molecular monolayer were immobilized at the electrode surface as detailed in ref 1. Then the regular step-by-step growth of the multimonolayer assembly was obtained by immersing successively the

(17) (a) In numerous papers dealing with the immunological step-by-step immobilization of one or several successive molecular monolayers of glucose oxidase−antibody conjugates,[7] it was ascertained that the reactivity of the immobilized enzyme is exactly the same as in solution.[7a] It was also shown that the enzyme reactivity is not significantly affected by the presence of PEG chains.[17b] (b) Anicet, N.; Anne, A.; Bourdillon, C.; Demaille, C.; Moiroux, J.; Saveant, J.-M. *Faraday Discuss.* **2000**, *116*, 269−279.

(18) Weibel, M. K; Bright, H. J. *J. Biol. Chem.* **1971**, *246*, 2734−2744.

(19) (a) Bourdillon, C.; Demaille, C.; Moiroux, J.; Savéant, J.-M. *J. Am. Chem. Soc.* **1993**, *115*, 2−10. (b) Alzari, P.; Anicet, N.; Bourdillon, C.; Moiroux, J.; Savéant, J.-M. *J. Am. Chem. Soc.* **1996**, *118*, 6788−6789.

(20) Bourdillon, C.; Demaille, C.; Moiroux, J.; Savéant, J.-M. *J. Am. Chem. Soc.* **1999**, *121*, 2401−2408.

modified electrode for 48 h in a 15 μg/mL solution of the relevant IgG species. The 48 h immersion time is required for efficient molecular recognition of IgG−PEG−Fc by anti-mouse antibodies or recognition of goat antigens by IgG−PEG−Fc, the presence of the PEG−Fc chains does not prevent molecular recognition, however it slows its rate down compared to molecular recognition between unlabeled antigens and antibodies. The self-assembly thus prepared was stored in the dark, at room temperature in PBS buffer plus sodium azide.

Cyclic Voltammetry. The instrumental setup was the same as previously described.[19a] The temperature in all experiments was 25 °C. All solutions were purged from dioxygen before each voltammetric run. Provided that prolonged overcompensation was avoided, the IgG assemblies did not suffer from the use of the ohmic drop compensation feedback loop. Thus reliable ohmic-drop free cyclic voltammograms could be recorded even at the highest potential scan rates we used. All potentials are referred to the KCl saturated calomel electrode (SCE).

Conclusions

The quantitative analysis of the catalytic efficiency of the wired redox enzyme confirms that, as soon as the enzyme-catalyzed reaction is relatively fast, the rate of electron transport through the protein assembly controls the kinetics of the integrated system. The overall rate of electron transport depends on N which controls the distance separating the immobilized monolayer of enzyme from the electrode surface, on n_i which characterizes the distance separating two successive IgG−PEG−Fc monolayers, on the dynamics of the PEG chains, and finally on the rate constant k_e of isotopic electron exchange between the Fc and Fc^+ heads.

The smaller N and n_i and the greater the mobility of the ferrocene heads and k_e, the faster the overall rate of electron transport. Those are qualitative conclusions which could have been intuitively anticipated. The step-by-step approach allowed by the immunological construction enabled us to control the spatial structure of the self-assembly of wired IgG's, and the model of elastic bounded diffusion enabled us to characterize quantitatively the effect of each parameter. The protein assembly being of low compactness and essentially aqueous, changes in solvent and ionic atmospheres accompanying oxidation or reduction of the mediator heads do not cause any swelling or contraction. The geometry of the protein assembly does not fluctuate, and the quantitative characterization of the structural parameters controlling the kinetics of the system can thus be carried out confidently.

Predictions concerning the effect of the fully stretched PEG chain length L_{fs} are not straightforward. At first glance one could think that the longer the fully stretched PEG chain the greater the chance to reach ferrocene heads of another IgG−PEG−Fc monolayer or enzyme active sites. Actually such a possibility of far reaching for the terminally attached ferrocene heads depends on both their spatial distribution at rest and the chain dynamics. The spatial distribution at rest is controlled essentially by the elastic penalty, that is the spring constant k_{spr}. It may thus seem that the length of the PEG chains does not matter, provided that the chains are long enough to allow the Gaussian distribution of the volume concentration of ferrocene heads attached to one IgG−PEG−Fc monolayer to reach practically zero on each side of the averaged anchoring plane of PEG chains into the IgG−PEG−Fc monolayer (see Figure 5). The energetic cost of extending the PEG chains beyond these limits is prohibitive. However the elastic penalty is of entropic origin and, in a good solvent, k_{spr} is practically proportional to $1/L_{fs}$;[21] therefore, an increase in L_{fs} will widen the Gaussian distribution and increase consequently the overall rate of electron transport. The dynamics of the PEG chains depends solely on the dimensionless parameter β which is proportional to k_{spr} and D. An increase in L_{fs} will cause a decrease in D that cannot be easily predicted,[10,21] the mobility of the PEG chains will slow, and the overall rate of electron transport will consequently slow.

For systems in which electron transport proceeds by electron hopping between redox mediators linked to one end of linear and flexible polymeric chains terminally attached, at the other end, to a regular network of anchoring points within an immobilized structure, it is not certain that the rate of electron transport can be improved dramatically compared to the system we elaborated and characterized in the present work. There exists no redox couple having much higher rate constant k_e than the Fc/Fc^+ couple.[16] The stiffness of saturated chains such as the PEG chains is low. Increasing the density of anchoring points of terminal attachment would give higher local volume concentrations of ferrocene heads. However, entanglement of the PEG chains could then become much more probable and interfere significantly. In consequence the apparent value of k_{spr} would increase while that of D would decrease, the net result being that the effective mobility of the ferrocene heads might not be much improved.

Supporting Information Available: Numerical solutions of the sets of differential equations in the absence and in the presence of enzyme (PDF). This material is available free of charge via the Internet at http://pubs.acs.org.

JA004050F

(21) (a) Pincus, P. *Macromolecules* **1976**, *9*, 386-388. (b) de Gennes, P. G. *Scaling Concepts in Polymer Physics*; Cornell University Press: Ithaca, New York, 1991; pp 29−53.